3D ordered macroporous NiO/Al nanothermite film with significantly improved higher heat output, lower ignition temperature and less gas production

Chunpei Yu[1], Wenchao Zhang[1,*], Ruiqi Shen[1], Xing Xu[1], Jia Cheng[1], Jiahai Ye[1], Zhichun Qin[1], Yimin Chao[2,*]

[1]School of Chemical Engineering, Nanjing University of Science and Technology, Nanjing, 210094, China

[2]School of Chemistry, University of East Anglia, Norwich, NR47TJ, United Kingdom

*Corresponding author, Tel: +86 84315515 Fax: +86 84315857

Email address: zhangwenchao@njust.edu.cn (W.C.) or y.chao@uea.ac.uk (Y.C.)

Abstract

The performances of nanothermites largely rely on a meticulous design of nanoarchitectures and the close assembly of components. Three-dimensionally ordered macroporous (3DOM) NiO/Al nanothermite film has been successfully fabricated by integrating colloidal crystal template (CCT) method and controllable magnetron sputtering. The as-prepared NiO/Al film shows uniform structure and homogeneous dispersity, with greatly improved interfacial contact between fuel and oxidizer at the nanoscale. The total heat output of 3DOM NiO/Al nanothermite has reached 2461.27 $J \cdot g^{-1}$ at optimal deposition time of 20 min, which is significantly more than the values of other NiO/Al structural systems that have been reported before. Intrinsic reduced ignition temperature (onset temperature) and less gas production render the wide applications of 3DOM NiO/Al nanothermite. Moreover,

this design strategy can also be readily generalized to realize diverse 3DOM structured nanothermites.

Keyword: nanothermite; NiO/Al; three-dimensionally ordered macroporous; magnetron sputtering; heat release

1. Introduction

Thermites are a class of energetic materials that compose of metal fuel (e.g. Al, Mg) and oxidizer (e.g. CuO, Fe_2O_3, MoO_3, NiO, Co_3O_4) [1-3]. Their intrinsic feature is to release heat, gas, and power rapidly upon the stimulus of thermal, electrical or optical actuation. Over the last decades, it has been demonstrated that thermites prepared in nanoscale are shown to be efficient in increasing heat release, reducing ignition delay and enhancing mechanical properties compared to their bulk or macro counterparts [4-9]. In addition, their properties can be tuned by controlling interface contact and optimum molar ratio of the two components [10]. Nanothermites have been applied in broad fields, such as microelectro-mechanical system (MEMS) [2, 11], thermal batteries, gas generators [12-14], and microthrusters [15, 16]. In some particular applications, for example microinitiators, little component vibration and short flow disturbance are required [17, 18]. Therefore, it is desirable to generate high heat output but little gas releasing from thermite reaction.

The gas generated by thermite reaction is mainly composed of the vapors of metals, the elemental oxygen from the oxidizer and other gaseous reaction products [19]. The quantity of gas produced in a particular reaction of composites depends on the thermodynamic properties of the reaction itself and the physical properties of the

reaction products [20]. If the reaction releases sufficient amount of heat to vaporize the intermediates and products, the gas released is to be enhanced. In numerous metal-oxide/Al thermites, the NiO/Al thermite exhibits excellent merit in terms of gas generation. Theoretically, the gas product from the NiO/Al thermite is 10^{-4} mol·g^{-1}, which is only 7.7% of those from Fe_2O_3/Al system and 2.0% from CuO/Al system [17]. Moreover, NiO/Al possesses a lower onset temperature than Fe_2O_3/Al [21] and CuO/Al [22, 23], which is a valuable advantage to reduce ignition delay. Therefore, it is important to carry out intense investigations on the NiO/Al thermite system.

Recently, there were some investigations on the preparation and properties of NiO/Al nanothermite [18, 19, 22]. In the literature, the composite of Al nanoparticles (Al-NPs) and NiO nanowires have been synthesized through ultrasonic mixing method, and the influence of NiO mass ratio over Al-NPs are widely discussed [19]. In this approach, owing to core-shell nanowires structure, the activation energy and onset temperature are reduced effectively. However the mixing homogeneity and effective contact area of NiO/Al composite are limited. These disadvantages lead to a relatively low energy output, 1000 J·g^{-1}, only 29% of the theoretical reaction heat from the NiO/Al system. In the work published by Zhang et al [18], the energy release is still low from nano-NiO/Al thermite film fabricated by electrophoretic deposition with controllable film thickness. This is induced by some inevitable impurities from the dispersion system. The study on a two-dimensional NiO/Al nano energetic material synthesized on a silicon substrate is another approach. The NiO nano honeycomb is produced by thermal oxidation of a Ni thin film and Al is directly

deposited via thermal evaporation [22]. This approach favors reducing ignition temperature, increasing interfacial contact area and compatibility with microsystems. However, the interspace among the NiO nano honeycomb is restricted, and Al deposited by thermal evaporation is insufficient, which is verified by the NiO peaks presented in the X-ray diffraction (XRD) pattern recorded after differential thermal analysis testing. Hence, new feasible fabrication methods are needed to prepare NiO/Al nanothermite with improved performances.

3DOM materials, hierarchically interconnected structures in three dimensions with extremely uniform pores [24], can act as a suitable carrier in composite materials. The highly porous structures and largely accessible surfaces [25] could ensure sufficient contact between the components of thermite. In our previous work, the Fe_2O_3/Al nanothermite films based on 3DOM Fe_2O_3 skeleton have successfully demonstrated this strategy for improving the thermites performance [26, 27]. The excellent 3DOM structure greatly enhances interfacial contact and mixing uniformity between fuel and oxidizer, which is leading to enhance the energy output.

In this study, a core/shell 3DOM NiO/Al nanothermite film is formed on 3DOM NiO skeleton prepared by CCT method with nano Al loaded using magnetron sputtering. To study the effect of molar ratio Al/NiO on the morphology and heat release, the 3DOM NiO/Al nanothermites are designed with three different deposition times. After the investigation on the thermo-chemical properties of the obtained samples, it is found that the maximum heat output of the optimized nanothermite film is 2461.27 $J \cdot g^{-1}$, which is significantly more than the values reported from other

structural NiO/Al systems.

2. Experimental section

2.1. Chemicals and materials

The chemical reagents of potassium persulfate (KPS, ≥99.5%), styrene(≥99%), sodium *p*-styrene sulfonate (≥98%), $NaHCO_3$ (≥99.5%), $Ni(NO_3)_2 \cdot 6H_2O$ (≥98%), anhydrous ethanol (≥99.7%), hydrochloric acid (36-38%), acetone (≥99.5%) and hexane (≥97%) were purchased from Sinopharm Chemical Reagent Co. Ltd., which were of analytical grade. NiO nanoparticles (NiO-NPs, ≥99.9%) and Al-NPs (≥99.9%) with an average size of 50 nm were supplied by Aladdin Industrial Corporation. Microslides (Nantong Fold Thai Experimental Instrumental Co. Ltd) were used as substrates.

2.2. Preparation of colloidal crystal template

Highly monodispersed polystyrene (PS) microspheres were synthesized via an emulsifier-free emulsion polymerization according to the previously reported method [26, 28, 29]. Polymerization of the styrene monomer was carried out in a four-necked bottom flask using KPS as the initiator. Briefly, 200 mL deionized water, 0.2 mmol sodium *p*-styrene sulfonate, 1.5 mmol $NaHCO_3$, 0.19 mol styrene monomer and 1.1 mmol KPS were successively introduced into the reactor. The whole polymerization system was stirred at approximately 300 rpm at 70^{o}C and purged with N_2. After 24 h, PS microspheres in the suspension were harvested. Afterwards, PS microspheres were orderly assembled on the microslide substrate via vertical deposition. Typically, completely clean microslide substrates (25 mm×38 mm) rinsed by hydrochloric acid,

acetone and anhydrous ethanol successively were immersed in the suspension of PS microspheres (1.5 vol %) vertically under a constant temperature of 45°C for 5 days. After the suspension dried up, PS CCT was then obtained.

2.3. Preparation of 3DOM NiO

The PS CCT was used to form 3DOM NiO skeleton. The precursor solution was prepared by dissolving 0.01 mol $Ni(NO_3)_2 \cdot 6H_2O$ in 10 mL of alcohol. Then, the mixture was magnetic stirring at room temperature for 4 h. The ordered PS CCT was firstly soaked vertically into the precursor solution for 5 min to form PS/precursor composite. Care was taken to keep the solution below the top of the PS CCT. After wiping off the excess solution, the impregnated template was dried for 4 h at 50°C in a drying oven up to solidification. Then, this process was repeated once more in order to ensure the PS CCT fully infiltrated. Finally, the resulting PS/NiO precursor composite was pyrolyzed in the air at 400°C for 1 h with a heating rate of 1 $°C \cdot min^{-1}$. The removal of PS microspheres and the formation of 3DOM NiO skeleton were simultaneously accomplished during calcination.

2.4. Preparation of 3DOM NiO/Al nanothermite

A layer of Al film was deposited over the internal surface of 3DOM NiO skeleton by magnetron sputtering to realize 3DOM NiO/Al nanothermite film. Ultrahigh purity Ar with a flow of 30 sccm acted as effective gas to bombard the Al target. In the process of deposition, the vacuum of the working chamber was maintained at 5×10^{-3} Pa and the temperature was maintained at 30°C. The rate of Al deposition was 0.5-1.0 $Å \cdot s^{-1}$. In order to explore the appropriate molar ratios of Al to 3DOM NiO and acquire

the best morphology and heat release of 3DOM NiO/Al nanothermite, the different deposition durations of 10 min, 20 min and 30 min were tested.

For comparison purpose, NiO-NPs/Al-NPs thermite and 3DOM NiO/Al-NPs thermite were prepared by classic ultrasonication mixing [30]. The Al-NPs were encapsulated within a protective Al_2O_3 shell. The active Al content was determined from weight-gain measurements by a thermal gravimetric analyzer (TGA) curve (see Fig. S1 in Supporting Information). Stoichiometric mixtures of the fuel and oxidizer components were obtained using hexane as the solvent and ultrasonication mixing for about 30 min to create a randomly mixed sample. Then the suspensions were dried at 65^{o}C for 6 h in order to obtain NiO-NPs/Al-NPs and 3DOM NiO/Al-NPs, respectively.

2.5. Characterization of samples

The crystal structures of obtained materials were analyzed by a Bruker D8 Advance XRD using Cu Kα radiation and nickel filter (λ=0.15406 nm). The morphologies of all the samples were characterized using a Hitachi S-4800 field emission scanning electron microscopy (FE-SEM). Simultaneously, energy dispersive X-ray spectrum (EDS) was used to explore the molar ratio of Al to NiO at different deposition times. The Brunauer-Emmett-Teller (BET) surface area of samples was measured by physisorption of N_2 at 77 K using a Quantachrome Autosorb-IQ gas adsorption analyzer. A Mettler Toledo differential scanning calorimetry (DSC) was used to determine the heat of reaction of the NiO/Al nanothermites from 300 to 900^{o}C at a heating rate of 20 ^{o}C·min^{-1} under a 30.0 mL·min^{-1} N_2 flow. The active Al content in

Al-NPs was calculated by a Mettler-Toledo TGA under air in the temperature range of 300-1000°C at a heating rate of 20 °C·min^{-1}. The ignition property of the nanothermite film was investigated by a Nd:YAG laser device. The wavelength, the pulse width and the incident laser energy were 1064 nm, 100 ns and 167 mJ, respectively. The whole ignition progress was monitored and recorded using a high-speed camera (Redlake Motion Xtra HG-100K) running at 5000 frames per second.

3. Results and discussion

3.1. Phase characterizations

The crystal structure and phase composition of the 3DOM NiO and 3DOM NiO/Al nanothermite film are investigated using XRD measurement. In Fig. 1(a), four sharp peaks at 37.25°, 43.28°, 62.88° and 75.41° are observed, which perfectly coincide with the standard card of bunsenite NiO (JCPDS card 47-1049), corresponding to planes of (111), (200), (220) and (311), respectively. Fig. 1(b) shows the XRD pattern of NiO/Al nanothermite. Except the peaks of NiO, three characteristic peaks at 38.47°, 44.74° and 65.13° of Al (JCPDS card 04-0787) are also identified. Meanwhile, there is no hint of impurities, which means that there is little or no reaction between NiO and Al under the high vacuum and sustained low temperature during magnetron sputtering.

3.2. Morphology characterizations

The morphologies of the PS CCT and the 3DOM NiO skeleton are examined by FE-SEM. In Fig. 2(a), the PS microspheres with the average diameter of 280 nm are arranged on the surface to form ordered close-packed arrays. Each PS microsphere is

surrounded by six others in hexagonal symmetry with the structure of face-centered cubic lattice [31], which is considered to be the most stable arrangement in thermodynamics [32]. The high-quality PS CCT is crucial for the further preparation of 3DOM NiO skeleton. The interstices between PS microspheres provide a favorable condition for the penetration of precursor via capillary effect. Fig. 2(b) shows the surface view of distinct 3DOM NiO skeleton, a high quality inverse copy of the PS CCT. The morphology of the skeleton consists of ordered hexagonal pores caused by the removal of previous PS microspheres. Through each pore on the top layer of the surface, three small pores in the next layer are observed, which ensure an interconnected structure in the whole skeleton. The wall thickness is approximately 30 nm. The average diameter of the pores is around 200 nm, corresponding to a pore shrinkage rate of about 28.6% from the original PS diameter. The deformation of the PS microspheres during the calcination is likely to be the main cause of this shrinkage [33]. The hierarchically interconnected structure and high porosity render the significantly specific surface area of this NiO film, which is 47.326 $m^2 \cdot g^{-1}$, as measured by BET analysis (see Fig. S2 in Supporting Information). Fig. 2 (c, d) show the corresponding cross-section view of the PS CCT and the 3DOM NiO skeleton, respectively. It is observed that the PS CCT has 10 layers, and the thickness is about 2.3 μm. In contrast, the thickness of 3DOM NiO skeleton is reduced to 1.9 μm after the PS microspheres are removed, which resulted from the incomplete filling of the precursor and the deformation of the PS CCT during the high-temperature calcination.

Our previous study revealed that magnetron sputtering offers controllable coverage

density of Al through adjusting deposition time [34]. Fig. 3 shows the SEM images of 3DOM NiO/Al nanothermite film formed at different deposition times. With the deposition time increasing, Al shell gets thicker and the pore diameter gets smaller. In comparison with SEM image of NiO skeleton, Fig. 2(b), NiO/Al nanothermite film at deposition time of 10 min in Fig. 3(a) reveals that the thickness of coated Al is about 80 nm. Fig. 3(b) shows that the pores of NiO skeleton are nearly sealed at deposition time of 20 min. When the deposition time is sequentially increased to 30 min, the pores are completely filled with Al and there is little excess Al on the surface. All the three top view images of 3DOM NiO/Al nanothermite film indicate that Al shell has been coated on NiO skeleton tightly and uniformly, which greatly reinforces the interfacial contact and improves the reactivity.

3.3. Elemental characterizations

Fig. 4 shows the EDS patterns of 3DOM NiO/Al film at different deposition times. Al and Ni peaks are both presented in the three patterns and it can be preliminarily obtained that the percentage of Al peak gets larger with deposition time increasing. Because of the treatment of spraying gold to improve conductivity, the element of Au also appears in spectrum patterns. After careful calculations, it is confirmed that the atomic percentages of Al in NiO/Al nanothermite films at different deposition times of 10 min, 20 min and 30 min are 3.72%, 27.89% and 26.64%, respectively. Similarly, the atomic percent of Ni are 7.15%, 30.53%, and 15.82%. Further calculation concludes that the molar ratios of Al to NiO in NiO/Al nanothermite films are 0.52, 0.91 and 1.68, respectively, corresponding to the deposition times of 10 min, 20 min

and 30 min. All calculation results are showed in Table 1. Obviously, the molar ratio of Al to NiO increases with the deposition time increase. It's worth noting that the stoichiometry for complete reaction of Al to NiO is 0.67, so Al is already in excess with the deposition time of 20 min. Fig. 4(d) shows the corresponding EDS mapping of 3DOM NiO/Al film at deposition time of 30 min, from which one can see that Al has been coated on NiO uniformly.

3.4. Thermal analysis

The thermite reaction of the NiO/Al system at the stoichiometric ratio is shown as

$$2Al + 3NiO \rightarrow Al_2O_3 + 3Ni \qquad \Delta Hr = 3.44\ kJ \cdot g^{-1}$$

The heat release of the 3DOM NiO/Al nanothermite film at different deposition times (10 min, 20 min and 30 min, respectively) is investigated by DSC. Only one exothermic peak with an onset temperature of 457.75^{o}C and a heat output of 948.89 $J \cdot g^{-1}$ is observed in Fig. 5(a), which is caused by the solid–solid reaction between the 3DOM NiO and the nano Al [22]. This phenomenon can be attributed to the fact that Al is insufficient at deposition time of 10 min. Fig. 5(b) shows the DSC curve of NiO/Al nanothermite at deposition time of 20 min. Two sharp exothermic peaks are observed with the heat output of 1103.50 $J \cdot g^{-1}$ and 1358.77 $J \cdot g^{-1}$, respectively. Note that the first heat output is already larger than that in Fig. 5(a), which further proves that the insufficient Al has been deposited at deposition time of 10 min. The second exothermic peak appears with the onset temperature of 645.24^{o}C, which is close to the melting point of Al (660^{o}C). Hence, the second exothermic reaction is largely caused by NiO and melted Al. Through calculation, integration of the two exothermic peaks

in the DSC gives a heat output of the reaction equal to 2461.27 $J \cdot g^{-1}$, possessing 71.5% of the theoretical value, which is the largest in our experiments. The molar ratio of Al to NiO in NiO/Al film at deposition time of 20 min is 0.91, which is above the theoretical value (0.66). Taking into consideration that some Al on the surface may have been oxidized before the DSC measurement during storage, therefore, an excess of Al is necessary to achieve the maximum heat output. With the deposition time increased to 30 min, there are also two exothermic peaks in Fig. 5(c). The heat output of the two exothermic reactions are 758.32 $J \cdot g^{-1}$ and 1004.88 $J \cdot g^{-1}$, respectively, which are correspondingly lower than the two heat output values of the sample that the deposition time is 20 min. This means that Al is considerably in excess. The total heat release with different deposition times changed obviously, but there is no significant change in the onset temperature of the first exothermic peak.

In order to make comparison, Fig. 5(d, e) show the DSC plots of the NiO-NPs/Al-NPs and 3DOM NiO/Al-NPs under the same test conditions, respectively. Two exothermic peaks are also observed in Fig. 5(d). Integration of the exothermic peaks in DSC curve gives a reaction heat of 895.0 $J \cdot g^{-1}$, which is much lower than that of 3DOM NiO/Al nanothermite film at the deposition time of 20 min, in spite of NiO-NPs and Al-NPs were mixed in the stoichiometric ratio. This further demonstrates that 3DOM structure combined with magnetron sputtering aluminizing significantly enhances energy output due to compact interfacial contact between fuel and oxidizer at the nanoscale. Moreover, it can be seen that the first onset temperature of 3DOM NiO/Al nanothermite film is approximately 65°C lower than that of

NiO-NPs/Al-NPs, which is very attractive for many applications that need nanothermites with low ignition temperature. In Fig. 5(e) the DSC profile from 3DOM NiO/Al-NPs is similar to that of NiO-NPs/Al-NPs, and also has two exothermic peaks in the corresponding positions. It is worth pointing out that the total heat release of 3DOM NiO/Al-NPs (808.8 $J \cdot g^{-1}$) is lower than the value of NiO-NPs/Al-NPs. Possible reason for this phenomenon is that Al-NPs cannot enter the internal channel of the 3DOM NiO skeleton via classic physical mixing, which causes relatively low dispersion (see Fig. S3 in Supporting Information).

Noting that the largest heat output of 3DOM structural NiO/Al nanothermite is 2461.27 $J \cdot g^{-1}$, which is increased by 260-1530 $J \cdot g^{-1}$ than those for previous NiO/Al systems [18, 19, 22]. The highly enhanced heat release of the nanothermite reaction may be attributed to the following three aspects. First, the 3DOM NiO/Al nanothermite film prepared by this method possesses uniform structure and homogeneous dispersity. The 3DOM NiO/Al composite film can be considered as an integration of countless independent nanothermite, which ensures that Al and NiO integrate compactly at the nanoscale. Second, impurities are efficiently avoided. Some unnecessary organics can be wiped out during calcination. Third, because of the high vacuum environment and low temperature during magnetron sputtering, the potential oxidization of Al and oxidation-reduction reaction between Al and NiO are significantly discounted.

3.5. Laser ignition

The ignition performance of 3DOM NiO/Al nanothermite film at deposition time of

20 min, is investigated via a Nd:YAG laser device and a HG-100K high speed camera. Fig. 6 is a series of pictures of the ignition results. It is observed that a dazzling white flash encircled by a nattier blue halo bursts out at 0.2 ms, after the laser pulse action on a piece of 3DOM NiO/Al film. The height of the flash is around 1 cm. With the flash down, the sparkles of yellow colour are observed at 0.6 ms due to the spattering of reaction products. The duration of the whole ignition process is 1.4 ms. The results have demonstrated that the 3DOM NiO/Al nanothermite film can be ignited successfully under the stimulus of laser pulse.

4. Conclusions

The 3DOM NiO/Al nanothermite film with uniform structure and homogeneous dispersity has been successfully synthesized using PS CCT method combined with magnetron sputtering. Through adjusting the deposition time to control the amount of nano Al coated on the NiO skeleton, the maximum heat output of the nanothermite film is 2461.27 $J \cdot g^{-1}$ at the optimal deposition time of 20 min, which is significantly higher than the values of other structural NiO/Al systems reported before. The compact interfacial contact between fuel and oxidizer fully guarantees the energy release. The realized 3DOM NiO/Al nanothermite film has other advantages of lowered ignition temperature and reduced impurities. Furthermore, the laser ignition experiment indicates that the 3DOM NiO/Al nanothermite film can be successfully ignited. Therefore, the 3DOM NiO/Al nanothermite has the great potential applications in the field of microinitiators. This method is also suitable for preparing diverse 3DOM metal oxide/Al nanothermites.

Acknowledgements

The authors are grateful for the financial support from National Natural Science Foundation of China (Grant 51576101), National Science Foundation of Jiangsu Province of China (Grant BK20141399), the Fundamental Research Funds for the Central Universities (Grant 30915012101) and the Priority Academic Program Development of Jiangsu Higher Education Institutions.

Reference

[1] L.L. Wang, Z.A. Munir, Y.M. Maximov. Thermite reactions: their utilization in the synthesis and processing of materials. J. Mater. Sci. 28 (1993) 3693-3708.

[2] C. Rossi, K. Zhang, D. Esteve, P. Alphonse, P. Tailhades, C. Vahlas. Nanoenergetic materials for MEMS: a review. J. Microelectrome. S. 16 (2007) 919-931.

[3] C. Rossi. Two decades of research on nano-energetic materials. Propell. Explos. Pyrot. 39 (2014) 323-327.

[4] S.H. Kim, M.R. Zachariah. Enhancing the rate of energy release from nanoenergetic materials by electrostatically enhanced assembly. Adv. Mater. 16 (2004) 1821-1825.

[5] C. Weir, M.L. Pantoya, M.A. Daniels. The role of aluminum particle size in electrostatic ignition sensitivity of composite energetic materials. Combust. Flame. 160 (2013) 2279-2281.

[6] Y. Ohkura, S.Y. Liu, P.M. Rao, X. Zheng. Synthesis and ignition of energetic CuO/Al core/shell nanowires. P. Combust. Inst. 33 (2011) 1909-1915.

[7] E.L. Dreizin. Metal-based reactive nanomaterials. P. Energ. Combust. 35 (2009) 141-167.

[8] Y. Yang, D. Xu, K. Zhang. Effect of nanostructures on the exothermic reaction and ignition of Al/CuOx based energetic materials. J. Mater. Sci. 47 (2011) 1296-1305.

[9] M. Petrantoni, C. Rossi, L. Salvagnac, V. Conedera, A. Esteve, C. Tenailleau, et al. Multilayered Al/CuO thermite formation by reactive magnetron sputtering: nano versus micro. J. Appl. Phys. 108 (2010) 084323.

[10] M. Bahrami, G. Taton, V. Conedera, L. Salvagnac, C. Tenailleau, P. Alphonse, et al. Magnetron sputtered Al-CuO nanolaminates: effect of stoichiometry and layers thickness on energy release and burning rate. Propell. Explos. Pyrot. 39 (2014) 365-373.

[11] G. Taton, D. Lagrange, V. Conedera, L. Renaud, C. Rossi. Micro-chip initiator realized by integrating Al/CuO multilayer nanothermite on polymeric membrane. J. Micromech. Microeng. 23 (2013) 3210-3216.

[12] K.S. Martirosyan, L. Wang, A. Vicent, L. Dan. Nanoenergetic gas-generators: design and performance. Propell. Explos. Pyrot. 34 (2009) 532-538.

[13] G.Q. Jian, L. Liu, M.R. Zachariah. Facile aerosol route to hollow CuO spheres and its superior performance as an oxidizer in nanoenergetic gas generators. Adv. Funct. Mater. 23 (2013) 1341-1346.

[14] K.S. Martirosyan, L. Wang, A. Vicent, D. Luss. Synthesis and performance of bismuth trioxide nanoparticles for high energy gas generator use. Nanotechnology. 20

(2009) 17579-17584.

[15] S.J. Apperson, A.V. Bezmelnitsyn, R. Thiruvengadathan, K. Gangopadhyay, S. Gangopadhyay, W.A. Balas, et al. Characterization of nanothermite for solid-fuel microthruster applications. J. Propul. Power. 25 (2009) 1086-1091.

[16] C.S. Staley, K.E. Raymond, R. Thiruvengadathan, S.J. Apperson, K. Gangopadhyay, S.M. Swaszek, et al. Fast-impulse nanothermite solid-propellant miniaturized thrusters. J. Propul. Power. 31 (2015) 483-483.

[17] G. Bohlouli-Zanjani, J.Z. Wen, A.M. Hu, J. Persic, S. Ringuette, Y.N. Zhou. Thermo-chemical characterization of a Al nanoparticle and NiO nanowire composite modified by Cu powder. Thermochimi. Acta. 572 (2013) 51-58.

[18] D. Zhang, X. Li. Fabrication and kinetics study of nano-Al/NiO thermite film by electrophoretic deposition. J. Phys. Chem. A. 119 (2015) 4688-4694.

[19] J.Z. Wen, S. Ringuette, G. Bohlouli-Zanjani, A. Hu, N.H. Nguyen, J. Persic, et al. Characterization of thermochemical properties of Al nanoparticle and NiO nanowire composites. Nanoscale. Res. Lett. 8 (2013) 1405-1410.

[20] S.W. Dean, M.L. Pantoya, A.E. Gash, S.C. Stacy, L.J. Hope-Weeks. Enhanced convective heat transfer in nongas generating nanoparticle thermites. J. Heat. Trans-T. Asme. 132 (2010) 2201-2210.

[21] N. Zhao, C. He, J. Liu, H. Gong, T. An, H. Xu, et al. Dependence of catalytic properties of Al/Fe_2O_3 thermites on morphology of Fe_2O_3 particles in combustion reactions. J. Solid. State. Chem. 219 (2014) 67-73.

[22] K. Zhang, C. Rossi, P. Alphonse, C. Tenailleau, S. Cayez, J.Y. Chane-Ching.

Integrating Al with NiO nano honeycomb to realize an energetic material on silicon substrate. Appl. Phys. A-Mater. 94 (2009) 957-962.

[23] K. Zhang, C. Rossi, G.A.A. Rodriguez, C. Tenailleau, P. Alphonse. Development of a nano-Al/CuO based energetic material on silicon substrate. Appl. Phys. Lett. 91 (2007) 113117.

[24] J. Zhang, L. Li, D. Liu, J. Zhang, Y. Hao, W. Zhang. Multi-layer and open three-dimensionally ordered macroporous TiO_2-ZrO_2 composite: diversified design and the comparison of multiple mode photocatalytic performance. Mater. Des. 86 (2015) 818-828.

[25] L. Zhi, X. Tan, G. Xin, L. Song. Synthesis of three-dimensionally ordered macroporous manganese dioxide-carbon nanocomposites for supercapacitors. J. Power. Sources. 267 (2014) 812-820.

[26] W. Zhang, B. Yin, R. Shen, J. Ye, J.A. Thomas, Y. Chao. Significantly enhanced energy output from 3D ordered macroporous structured Fe_2O_3/Al nanothermite film. ACS. Appl. Mater. Inter. 5 (2013) 239-242.

[27] G. Zheng, W. Zhang, X. Xu, R. Shen, J. Deng, Y. Ye. Preparation of porous core/shell structure Fe_2O_3/Al nanothermite membrane by template method. J. Inorg. Mater. 30 (2015) 610-614.

[28] G.I.N. Waterhouse, M.R. Waterland. Opal and inverse opal photonic crystals: Fabrication and characterization. Polyhedron. 26 (2007) 356-368.

[29] C.E. Reese, C.D. Guerrero, J.M. Weissman, K. Lee, S.A. Asher. Synthesis of highly charged, monodisperse polystyrene colloidal particles for the fabrication of

photonic crystals. J. Colloid. Interf. Sci. 232 (2000) 76-80.

[30] J.L. Cheng, H.H. Hng, Y.W. Lee, S.W. Du, N.N. Thadhani. Kinetic study of thermal- and impact-initiated reactions in Al-Fe_2O_3 nanothermite. Combust. Flame. 157 (2010) 2241-2249.

[31] J.H. Kim, S.H. Kang, K. Zhu, J.Y. Kim, N.R. Neale, A.J. Frank. Ni-NiO core-shell inverse opal electrodes for supercapacitors. Chem. Commun. 47 (2011) 5214-5216.

[32] Z. Cheng, William B. Russel, P.M. chaikin. Controlled growth of hard-sphere colloidal crystals. Nature. 401 (1999) 893-895.

[33] Y. Xia, B. Gates, Y. Yin, Y. Lu. ChemInform abstract: monodispersed colloidal spheres: old materials with new applications. Adv. Mater. 12 (2000) 693-713.

[34] G. Zheng, W. Zhang, R. Shen, J. Ye, Z. Qin, Y. Chao. Three-dimensionally ordered macroporous structure enabled nanothermite membrane of Mn_2O_3/Al. Sci. Rep-UK. 6 (2016) 22588.

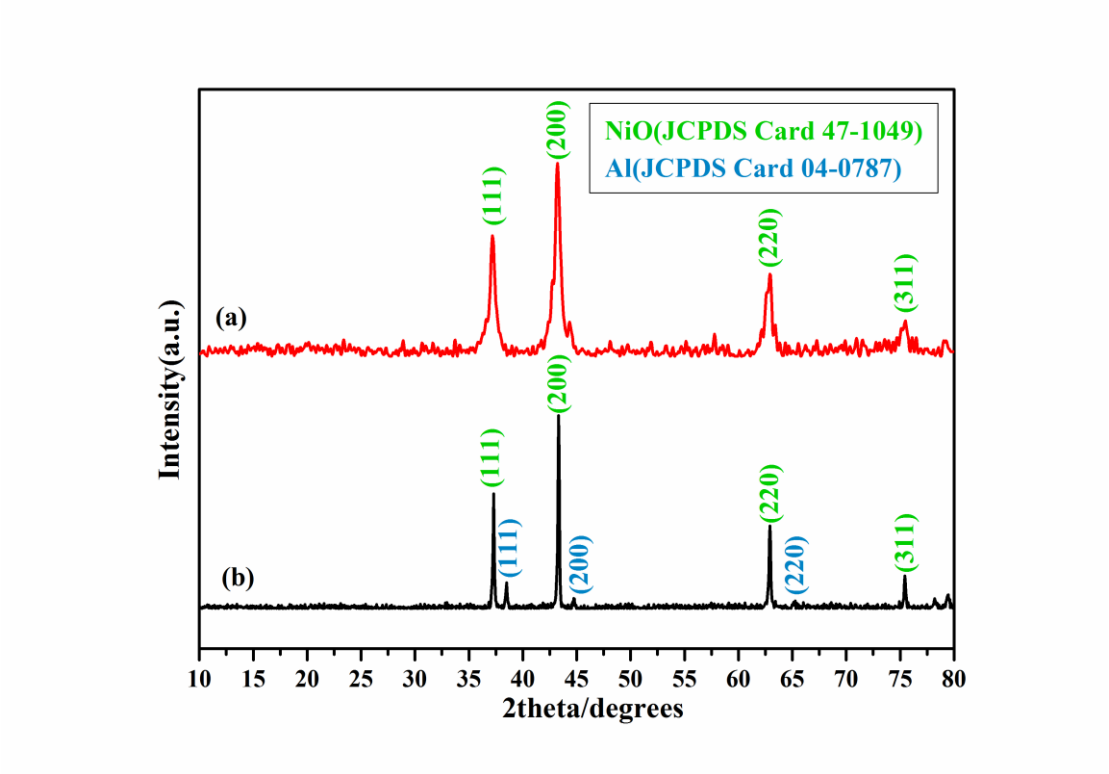

Fig. 1 XRD patterns of (a) 3DOM NiO skeleton and (b) 3DOM NiO/Al nanothermite film

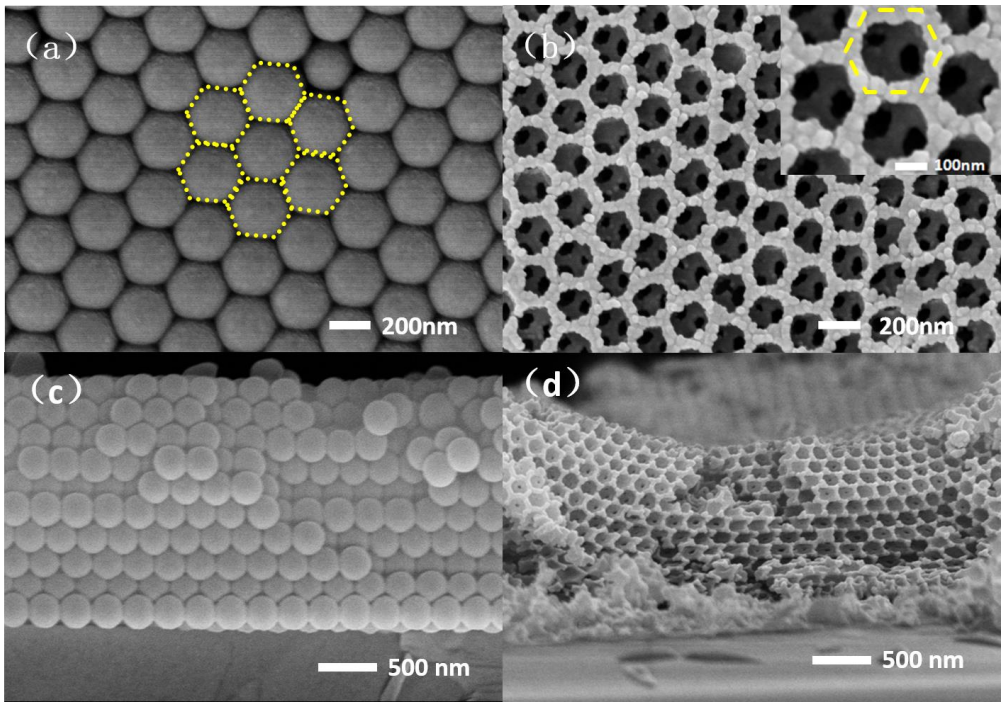

Fig. 2 SEM images of (a, c) PS CCT, (b, d) 3DOM NiO skeleten; (a, b) surface view and (c, d) cross-section view

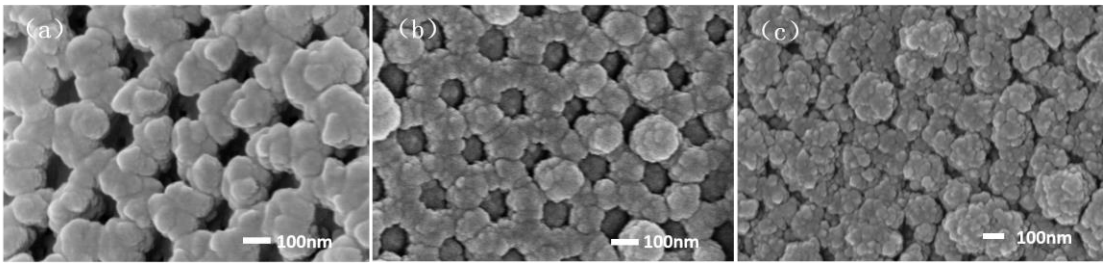

Fig. 3 SEM images of 3DOM NiO/Al nanothermite film at different deposition times, (a) 10 min; (b) 20 min; (c) 30 min

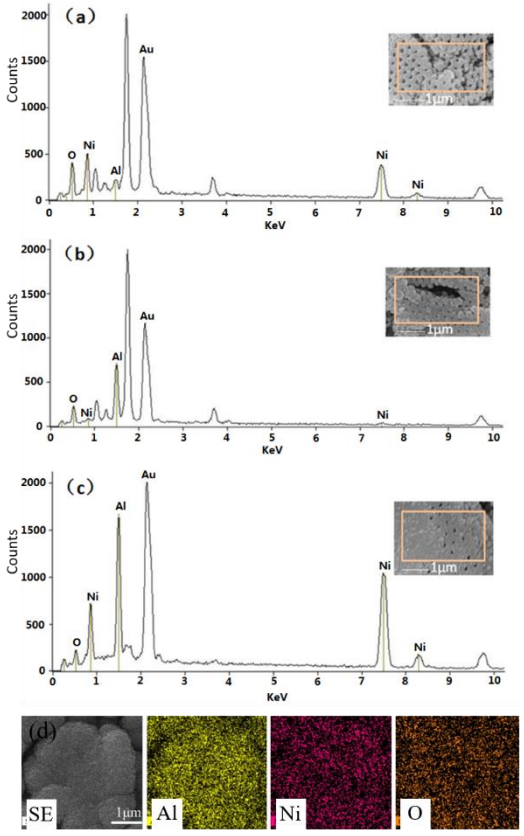

Fig. 4 EDS of 3DOM NiO/Al film at different deposition times, (a) 10 min; (b) 20 min; (c) 30 min;(d) corresponding EDS mapping of 3DOM NiO/Al film at the deposition time of 30 min

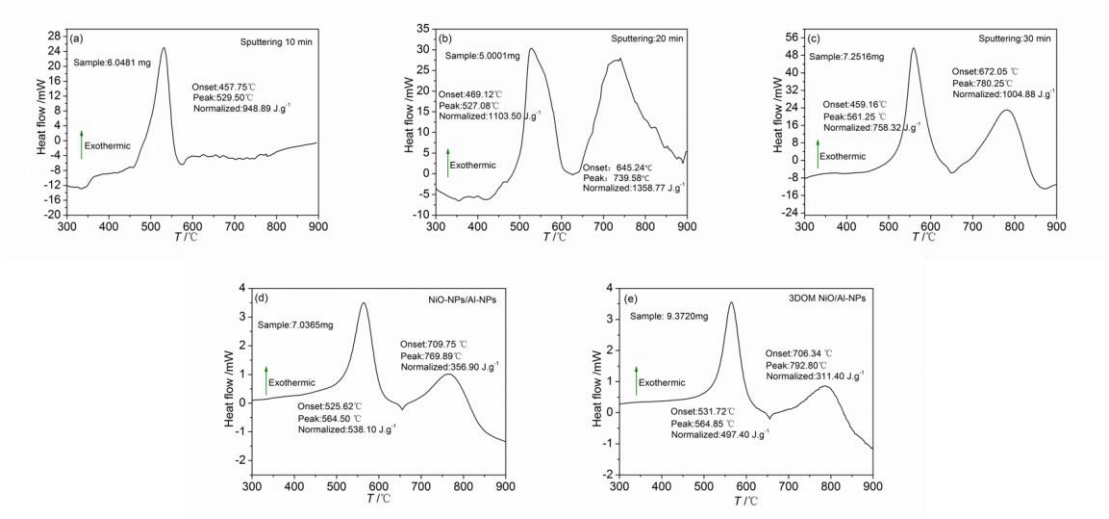

Fig. 5 DSC curve of 3DOM NiO/Al nanothermite film at different deposition times (a) 10min; (b) 20min; (c) 30min; DSC curves of (d)NiO-NPs/ Al-NPs and (e)3DOM NiO/ Al-NPs

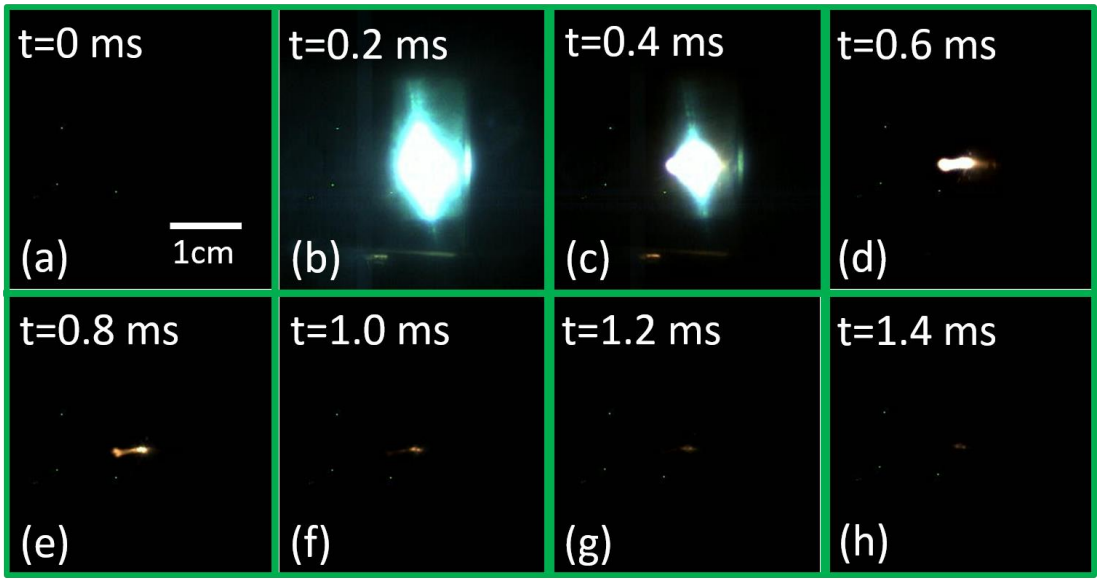

Fig. 6 High speed camera images of laser ignition process of 3DOM NiO/Al nanothermite film at the deposition time of 20 min

Table 1 Elemental composition of the 3DOM NiO/Al films with different deposition times

Deposition time (min)	Atomic percentage of the elements (%)		Molar ratio of Al to NiO
	Al	Ni	
10	3.72	7.15	0.52
20	27.89	30.53	0.91
30	26.64	15.83	1.68

Graphical abstract

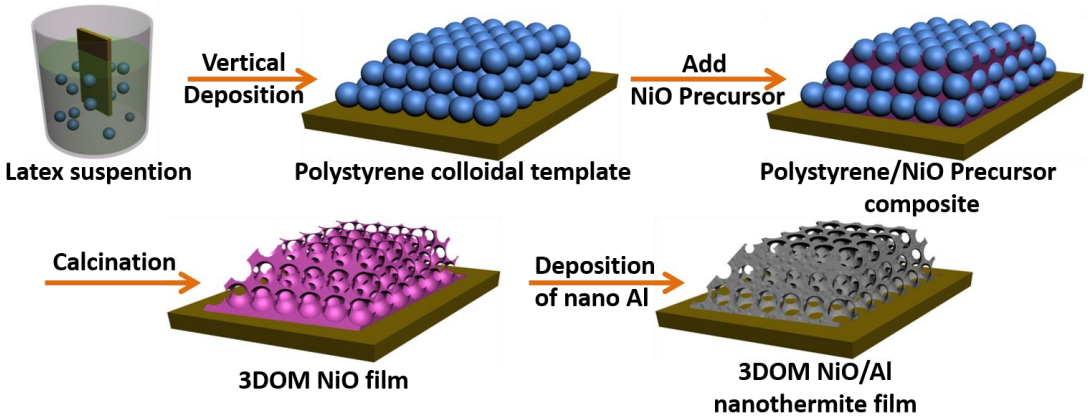

Highlights

1. Three-dimensionally ordered macroporous NiO/Al nanothermite film has been obtained by integrating colloidal crystal template method and controllable magnetron sputtering.

2. The morphology and heat release of the designed nanomaterials can be controlled by different aluminizing times.

3. This nanothermite significantly enhances energy output, possessing 71.5% of the theoretical value, which is increased by 260-1530 $J \cdot g^{-1}$ than those for other structural NiO/Al systems.

4. Obtained NiO/Al system exhibits advantages of lowered ignition temperature (about 460°C), reduced impurities and less gas production.

5. This NiO/Al nanothermite film has the great potential applications in the field of microinitiators.